Experimental study of the transformation of smectite at 80 and 300°C in the presence of Fe oxides

D. Guillaume, A. Neaman, M. Cathelineau, Régine Mosser-Ruck, C. Peiffert, Mustapha Abdelmoula, J. Dubessy, F. Villieras, N. Michau

Clay Minerals (2004) **39**, 17–34

Experimental study of the transformation of smectite at 80 and 300ºC in the presence of Fe oxides

D. GUILLAUME[1,*], A. NEAMAN[2], M. CATHELINEAU[1], R. MOSSER-RUCK[1], C. PEIFFERT[1], M. ABDELMOULA[3], J. DUBESSY[1], F. VILLIÉRAS[2] AND N. MICHAU[4]

[1] *Géologie et Gestion des Ressources Minérales et Energétiques (G2R), UMR 7566 CNRS-CREGU-INPL-UHP, Université Henri Poincaré, BP 239, 54506 Vandœuvre-lès-Nancy,* [2] *Laboratoire Environnement et Minéralurgie (LEM), UMR 7569 CNRS-INPL, Ecole Nationale Supérieure de Géologie, BP 40, 54501 Vandœuvre-lès-Nancy,* [3] *Laboratoire de Chimie Physique et Microbiologie pour l'Environnement (LCPME), UMR 7564 CNRS-UHP, Université Henri Poincaré, 405 rue de Vandœuvre, 54600 Villers-lès-Nancy,* [4] *Agence nationale pour la gestion des déchets radioactifs (ANDRA), Direction Scientifique/Service Matériaux, Parc de la Croix Blanche, 1/7 rue Jean Monnet, 92298 Châtenay-Malabry, France*

(*Received 6 January 2003; revised 26 July 2003*)

ABSTRACT: The alteration and transformation behaviour of montmorillonite (Wyoming bentonite) was studied experimentally to simulate the mineralogical and chemical reaction of clays in contact with steel in a nuclear waste repository. Batch experiments were conducted at 80 and 300ºC, in low-salinity solutions (NaCl, $CaCl_2$) and in the presence or otherwise of magnetite and hematite, over a period of 9 months. The mineralogical and chemical evolution of the clays was studied by XRD, SEM, transmission Mössbauer spectroscopy and EDS-TEM. Experimental solutions were characterized by ICP-AES and ICP-MS. The main results are that no significant change in the crystal chemistry of the montmorillonite occurred at 80ºC, while at 300ºC, the presence of Fe oxides leads to a partial replacement of montmorillonite by high-charge trioctahedral Fe^{2+}-rich smectite (saponite-like) together with the formation of feldspars, quartz and zeolites.

KEYWORDS: bentonite, smectite, saponite, magnetite, hematite, experimental synthesis, EDS-TEM, transmission Mössbauer spectroscopy, X-ray diffraction.

Numerous data are available from the literature on the experimental behaviour of smectites under hydrothermal conditions, generally in the presence of chloride solutions (e.g. Eberl, 1978; Eberl *et al*., 1978; Yamada *et al*., 1998). Iron is present in a variety of environments under several types of mineral phases: oxides (mostly hematite) or sulphides in clay-rich mudrocks, steel and its related oxidation products (goethite, lepidocrocite) in underground works (artificial barriers, tunnels, etc.). The availability of Fe in a solution-clay system depends mostly on the oxidation-reduction conditions and needs to be considered to predict the evolution of both natural systems and those disturbed by human activities: in this case, clay barriers in nuclear waste disposal. Although hematite-magnetite is probably not acting as an oxygen buffer at low temperatures, the presence of Fe oxides together with chloride solutions under intermediate redox conditions (from a theoretical f_{O_2} value typical of hematite-magnetite equilibrium to values expected in systems purged of significant

* E-mail: damien.guillaume@g2r.uhp-nancy.fr
DOI: 10.1180/0009855043910117

oxygen reserve) is important to consider for the prediction of the mineralogical evolution of the Fe-smectite-chloride solution system. Some qualitative description of the evolution of Fe-rich clays in natural systems such as the alteration of the oceanic crust is relatively well known (e.g. Buatier *et al*., 1989, 1993, 1995). However, only few experimental data are available on a smectite/Fe oxides (hematite + magnetite) system.

The review by Madsen (1998) carried out under conditions close to those of nuclear waste disposal mentions an experimental study of the bentonite-magnetite systems at 80ºC up to 29 weeks under low pressure ($P < P$ sat. H_2O vapour, Müller-Vonmoos *et al*., 1991). No change in the mineralogy, interlayer charge and cation exchange capacity (CEC) of the samples was detected. Minor changes are probably partly due to the fact that no free water was added to the system, the water being mostly under vapour phase, thus inhibiting significantly the dissolution of minerals and mineral-water reactions.

In the present study, experiments have investigated the hydrothermal stability of a bentonite at 80 and 300ºC in the presence of magnetite, hematite and chloride solutions under saturated vapour conditions. Analytical investigations concern both solid and liquid phases.

MATERIALS AND METHODS

Starting material

The MX80 bentonite (Na/Ca-bentonite, Wyoming), referred to as 'starting bentonite', was used for the experiments. It has a CEC of 79 mEq/100 g (Table 1) and the following composition (Guillaume *et al*., 2001a): montmorillonite (79%), quartz (3%), K-feldspars (2%), plagioclases (9%), carbonates (2%), mica (3%) and other minerals (mostly pyrite, phosphates and hematite, 2%). The crystal chemistry of the montmorillonite (<2 μm fraction of the bentonite) is based on microprobe analyses that are in good agreement with EDS and ICP-MS analyses. Taking into account an Fe^{3+}/Fe_{tot} ratio determined by transmission Mössbauer spectroscopy and EELS-TEM (Guillaume *et al*., 2001b), the structural formula is:

$$(Si_{3.98}Al_{0.02})(Al_{1.55}Mg_{0.28}Fe^{III}_{0.09}Fe^{II}_{0.08})O_{10}(OH)_2Na_{0.18}Ca_{0.10} \quad (1)$$

Preparation of the starting solid-solution system

The solution was prepared from analytical-grade chemicals. A Milli-Q Reagent Water System from Millipore Corp. provided deionized water (DI) with a resistivity >18 MΩ cm^{-1}. Na^+ and Ca^{2+} chlorides were added to de-ionized water to simulate the Na^+/Ca^{2+} ratio of natural water in sediments which in general is between 10 and 100. The starting solution contained 0.0207 mol/kg NaCl and 0.0038 mol/kg $CaCl_2$ and the total chloride concentration was 0.0282 mol/kg. Bentonite (1.5 g) was added to the solution with a liquid/solid mass ratio of 10. Then, in the case of experiments carried out in the presence of added Fe oxides, magnetite and hematite powders were added with an Fe/bentonite mass ratio of 0.1 and a magnetite/hematite mass ratio of 1. Argon was bubbled throughout the

TABLE 1. CEC (mEq/100 g) of the starting bentonite and run samples as a function of experimental conditions.

	Sample	CEC
	Starting bentonite	79
'Bentonite' samples		
25ºC	Starting sample	79
80ºC	1 week	n.a.
	1 month	n.a.
	3 months	73
	9 months	78
300ºC	1 month	n.a.
	9 months	73
'Mt-Hm' samples		
25ºC	Starting sample	70
80ºC	1 week	n.a.
	1 month	n.a.
	3 months	64
	9 months	72
300ºC	1 week	n.a.
	1 month	n.a.
	3 months	71
	9 months	62

'Bentonite' samples: experiments performed in the presence of bentonite and Na/Ca solution.
'Mt-Hm' samples: experiments performed in the presence of bentonite, Na/Ca solution and the addition of magnetite and hematite. Na/Ca solution: experimental solution containing 0.0207 mol/kg NaCl and 0.0038 mol/kg $CaCl_2$
n.a.: not analysed

solution-clay suspension over a period of 45 min to obtain an oxygen-free system and the preparation was equilibrated at room temperature for 6 days. The solution pH was then measured using a Mettler® combination pH electrode at 25ºC, and the Na^{+}/Ca^{2+} ratio of the reacting solution was around 75 (±2) as a result of exchange processes. Two types of solid assemblages were used at 80 and 300ºC: (1) bentonite with no Fe oxide added (samples named 'Bentonite 80' and 'Bentonite 300'); (2) bentonite with added magnetite and hematite powders (samples named 'Mt-Hm 80' and 'Mt-Hm 300').

Experimental procedure

The experimental conditions are listed in Table 1. The starting solids and solution mixture were mounted, under argon atmosphere, inside autoclaves. Teflon-lined autoclaves (capacity ~24 ml) were used for the 80ºC experiments and gold-lined warm-seal autoclaves (capacity ~18 ml) for the 300ºC experiments. The gold liner is mechanically sealed by a gold disc when the autoclave is closed by bolting. The autoclaves are then heated up to 80 and 300ºC in two furnaces. The internal pressure is the liquid-vapour equilibrium pressure at 80 or 300ºC. The durations of the experiments were 1 week, 1, 3 and 9 months. The temperature control was stable to ~2ºC. The vessels were removed at specific time intervals, quenched at 25ºC and opened under argon atmosphere. Run-samples were collected under argon atmosphere and centrifuged to extract the solution. Solution aliquots were taken, measured for pH and Eh and filtered through 0.45, then 0.02 μm, filters into cleaned polypropylene bottles and analysed. The solid was dried under argon flux at room temperature and gently ground in a mortar. Run samples were then stored in hermetically closed boxes under argon atmosphere until they were analysed. Solids were suspended again in pure water for the preparation of oriented mounds for XRD, or in methanol for the preparation of TEM grids.

X-ray diffraction (XRD)

The XRD data were collected using a D8 Bruker diffractometer with Co-$K\alpha_1$ radiation (λ = 1.7902 Å). The XRD patterns of unoriented powders were obtained in order to identify non-clay minerals. The XRD analysis was also carried out for the air-dried and ethylene glycol (EG)-saturated oriented specimens of the <2 μm fractions of the starting- and run-samples. The Greene-Kelly (Hoffmann-Klemen) test was performed (Greene-Kelly, 1953; Hoffmann & Klemen, 1950). The <2 μm fraction of each run sample was Li saturated, heated at 400ºC overnight and then glycerol saturated. Pure silica slides were used for oriented specimens of Li-saturated samples to avoid Na migration from the glass (Byström-Brusewitz, 1975). Additional treatments included (1) K saturation, heating at 110ºC overnight followed by EG saturation, (2) Mg saturation and glycerol-saturation, and (3) Li saturation then EG saturation.

Cation exchange capacity (CEC)

The CECs of the starting and run samples were determined as follows. Samples were Ba^{2+} saturated by treating three times with 1 N $BaCl_2$ solution, washed with distilled water and centrifuged until the electrical conductivity of the equilibrium solution was <10 $\mu\Omega\ cm^{-1}$. Ba^{2+} was then exchanged by treating the samples three times with 1 N $NaNO_3$ solution. Ba^{2+} concentrations in the solutions were determined by atomic absorption spectrometry.

Scanning electron microscopy (SEM)

Scanning electron micrographs were obtained using an Hitachi S-2500 Fevex scanning electron microscope. The denser fraction of each sample was separated by successive ultrasonication and sedimentation in alcohol, then disposed on carbon adhesive sticks. Semi-quantitative chemical analyses were also performed. The separated <2 μm fraction of each run sample was also examined to check the nature of newly formed non-clay minerals intimately associated with the clay.

Transmitted Mössbauer spectroscopy (TMS)

Transmission Mössbauer spectra were collected using a constant-acceleration spectrometer with a 50 mCi source of ^{57}Co in Rh. The spectrometer was calibrated with a 25 μm foil of α-Fe at room temperature. Spectra were obtained at 12 K or 150 K. The cryostat consisted of a closed-cycle helium Mössbauer cryogenic workstation with vibrations isolation stand manufactured by Cryo

Industries of America. Helium exchange gas was used to thermally couple the sample to the refrigerator, allowing variable temperature operation from 12 to 300 K. The samples were set in the sample holder in a glove box filled with an Argon atmosphere and quickly transferred in the cryostat for Mössbauer measurements. Computer fittings are performed by using Lorentzian-shape lines. The parameters that results from any computer fitting must be both mathematically (χ^2 minimization) and physically significant; in particular the width of all lines must be small enough (Benali *et al*., 2001).

Energy dispersive spectroscopy (EDS-TEM)

Micro-chemical analyses of isolated clay particles of the <2 μm fraction were obtained with an EDAX energy dispersive X-ray analyser attached to a CM20-Philips® instrument operating at 200 kV equipped with Si-Li detector and Li super ultra-thin windows (SUTW). Spectra were collected under nanoprobe mode, over a period of 40 s from an area ~10 nm in diameter. Elemental composition was calculated assuming the thin-film criteria (SMTF program: semi-quantitative metallurgical thin film program) and using k-factors calibrated with independently analysed macroscopic micas, with a maximum error of 5% for each element. 30 to 50 analyses were performed on isolated particles for each sample. The structural formula was calculated for each analysed particle taking into account the Fe^{3+}/Fe_{tot} ratio determined using TMS.

Analyses of run solutions

Chemical analyses of the experimental solutions were obtained by ICP-AES (Na^+, K^+, Ca^{2+}, Mg^{2+}, Fe^{2+} and Si^{4+} concentrations) and ICP-MS (Al^{3+} concentration). Solutions were acidified to avoid

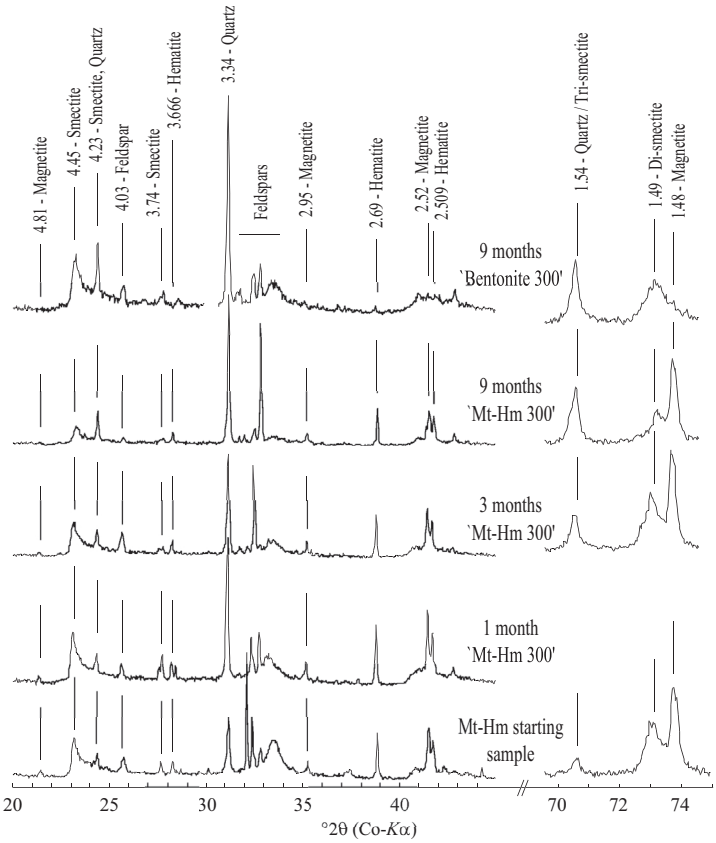

FIG. 1. XRD powder patterns of the Mt-Hm starting sample, 1 month, 3 months and 9 months 'Mt-Hm 300' run samples, and 9 months 'Bentonite 300' run sample. Reflection values in Å.

precipitation of Al or Fe hydroxides and diluted to bring concentrated analytes into quantification ranges of the ICP-AES and ICP-MS techniques. Because hydrochloric acid and sulphuric acid form poly-atomic species, nitric acid was chosen as the acidifying solution for both ICP-AES and ICP-MS analyses at 1.5%w/v and 3%w/v, respectively. The accuracy in measured solution concentrations was ±10%.

RESULTS

Mineralogy of the added Fe-bearing phases

The magnetite and hematite powders added to the starting samples were detected by both XRD and SEM in all the run samples. No significant difference in the relative intensity of magnetite and hematite reflection lines was detected between the starting and run samples (Fig. 1), indicating that the amount of magnetite and hematite in the sample did not change significantly. However, the size of magnetite and hematite crystals observed with SEM is modified. The starting powders were made of <5 μm grains (Fig. 2a). After the 9 month experiments, 40–200 μm euhedral magnetite and hematite crystals were observed in the run samples (Fig. 2b). In the case of 'Bentonite' experiments, the trace amounts of Fe oxides present in the starting sample were not observed in the run samples.

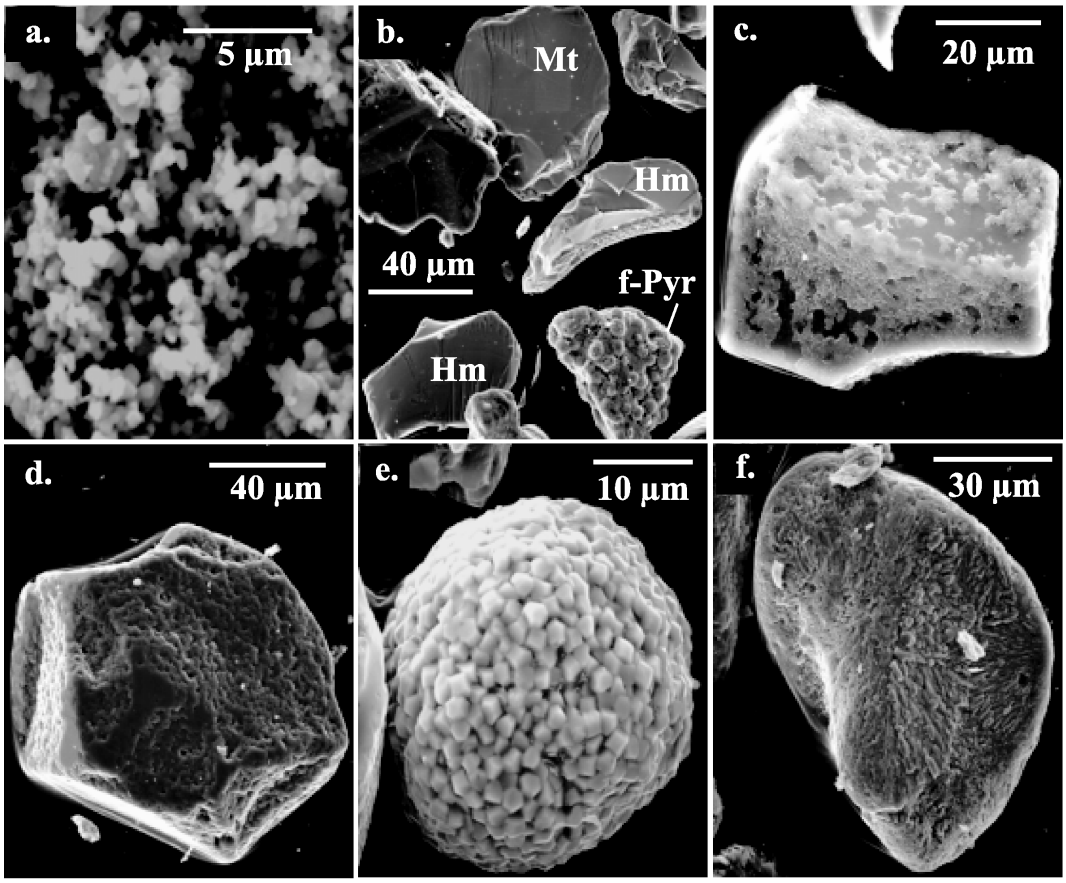

FIG. 2. Evolution of the morphology of primary minerals as seen by SEM: (a) hematite powder used in the Mt-Hm starting sample; (b) hematite and magnetite crystals observed in the 9 months 'Mt-Hm 80' run sample; (c) overgrowth of quartz in the 3 months 'Mt-Hm 80' run sample; (d) overgrowth of albite in the 9 months 'Bentonite 300' run sample; (e) framboidal pyrite in the starting bentonite, (f) partly dissolved pyrite in the 9 months 'Bentonite 300' run sample.

TABLE 2. Assemblage of non-clay minerals in the starting bentonite (Guillaume *et al*., 2001a) and as observed by SEM in the starting and run samples.

Sample		Qz	Fk	Plagio	Carb	Phos	Pyr	Mica	Mt	Hm
Starting bentonite		3%	2%	9%	2%	+	+	3%		+
'Bentonite' samples										
25ºC	Starting	+	+	+	+	+	+	+	n.o.	+
80ºC	3 months	+ Gr	+ Gr	+ Gr	+	+	+	+	n.o.	+
	9 months	+ Gr	+ Gr	+ Gr	n.o.	n.o.	+	+	n.o.	n.o.
300ºC	1 month	+ Gr	+ Gr	+ Gr	n.o.	n.o.	+	n.o.	n.o.	n.o.
	9 months	+ Gr	+ Gr	+ Gr	n.o.	n.o.	−	n.o.	n.o.	n.o.
'Mt-Hm' samples										
25ºC	Starting	+	+	+	+	+	+	+	+	+
80ºC	3 months	+ Gr	+ Gr	+ Gr	+	+	+	+	+	+
	9 months	+ Gr	+ Gr	+ Gr	+	+	+	n.o.	+	+
300ºC	1 month	+ Gr	+ Gr	+ Gr	n.o.	n.o.	n.o.	n.o.	+	+
	3 months	+ Gr	+ Gr	+ Gr	n.o.	n.o.	n.o.	n.o.	+	+
	9 months	+ Gr	+ Gr	+ Gr	n.o.	n.o.	n.o.	n.o.	+	+

+: presence of the mineral; Gr: evidence of growth or neoformation; −: evidence of dissolution; n.o.: mineral not present; Qz: quartz, Fk: K-feldspars, Plagio: plagioclase, Carb: carbonate, Phos: phosphate, Pyr: pyrite, Mt: magnetite, Hm: hematite.

Mineralogy of the other non-clay phases

The results of examination by SEM are summarized in Table 2. There was evidence for growth of quartz (or cristobalite), K-feldspars and plagioclases in the detrital fraction of all run samples. Figures 2c and 2d show overgrowths of quartz (or cristobalite) and plagioclase (albite), respectively. Carbonate, phosphate and mica that were present in the starting sample were no longer observed in either the 'Bentonite 300' or 'Mt-Hm 300' run samples. Pyrite that was present in the starting bentonite (Fig. 2e) is not observed in the

TABLE 3. Summary of the results of XRD analyses for the 00*l* spacing of the starting and run samples.

Sample		Type of treatment for XRD analysis Or	EG	Li sat	G-K test	K sat	Mg sat
'Bentonite' samples							
25ºC	Starting	12.6(s); 15.3(sh)	17.1	12.4	9.4		n.a.
80ºC	3 months	12.5(s)	17.1	12.5	9.2	n.a.	n.a.
	9 months	12.6(s); 15.2(sh)	17.1	12.4	9.1	n.a.	n.a.
300ºC	9 months	12.7(s); 14.9(s)	17.1	12.4	8.8; 16.7	13.9(sh);16.0(s)	17.0
'Mt-Hm' samples							
25ºC	Starting	12.7(s); 14.5(sh)	17.1	12.5	9.3	16.7	n.a.
80ºC	3 months	12.5(s)	17.3	12.4	9.3	n.a.	n.a.
	9 months	12.5(s)	17.3	12.4	9.1	n.a.	n.a.
300ºC	1 month	12.5(s); 14.9(sh)	n.a.	n.a.	n.a.	n.a.	n.a.
	3 months	12.6(s); 14.9(s)	17.1	12.4	8.9; 16.7	n.a.	n.a.
	9 months	12.7(s); 14.8(s)	17.0	12.4	8.6; 17.0	13.9	17.0

Treatment abbreviations: Or: oriented; EG: ethylene-glycol saturated; Li sat: Li saturated; G-K test: Greene-Kelly test; K sat: K saturated, then heated at 110ºC overnight and EG saturated; Mg sat: Mg then glycerol saturated. (s): strong reflection line, (sh): shoulder,
n.a.: not analysed

'Mt-Hm 300' run sample. There was evidence of pyrite dissolution in the 9 months 'Bentonite 300' run sample (Fig. 2f). Observations by SEM of the <2 μm fraction of the 9 months 'Bentonite 300' and 'Mt-Hm 300' run samples demonstrated the presence of newly formed zeolite associated with clay particles. Precise determination of the nature of these zeolite particles was not possible from semi-quantitative chemical analyses on SEM. They are mostly sodic with Si/Al ratio ranging from 2.25 to 3, close to phillipsite or stilbite composition. Based on SEM and XRD observations, zeolite was not present in the starting bentonite.

Significant increase in relative intensities of quartz reflection lines was detected in the run-samples of both 'Bentonite' and 'Mt-Hm' experiments treated at 300ºC (Fig. 1). In the case of 80ºC run samples, no significant change in the relative intensities of quartz reflection lines was observed.

Mineralogy of the clay phase

XRD results – transformation of the montmorillonite in the presence of magnetite and hematite at 300ºC ('Mt-Hm 300' run samples). The results of the XRD analyses for 00*l* spacing of the starting and run samples are summarized in Table 3. Oriented slides were prepared for the Mt-Hm starting sample and the 1, 3 and 9 months run samples. The XRD patterns obtained before and after EG saturation are presented in Fig. 3. They show, for air-dried specimens and increasing duration of experiment, a slight decrease of the 12 Å peak (characteristic of the presence of a monovalent cation) and a new reflection at 14.9 Å (characteristic of the presence of a divalent cation) the intensity of which increases, especially after 3 months. This indicates that the starting sodic smectite became progressively sodi-calcic, and then mostly calcic after 9 months. All the run samples expand to ~17 Å after EG saturation, indicating that expandable layers of smectite type remain predominant.

The XRD patterns from the Greene-Kelly test carried out on the same samples are presented in Fig. 4. The reflection line at 9.3 Å for the starting sample is attributed to a collapsed montmorillonite, and the intense reflection line at 17 Å in the 9 months run sample is attributed to the presence of a tetrahedral charge deficiency. The 3 months run sample shows intermediate features, in particular the presence of the two above-mentioned reflection

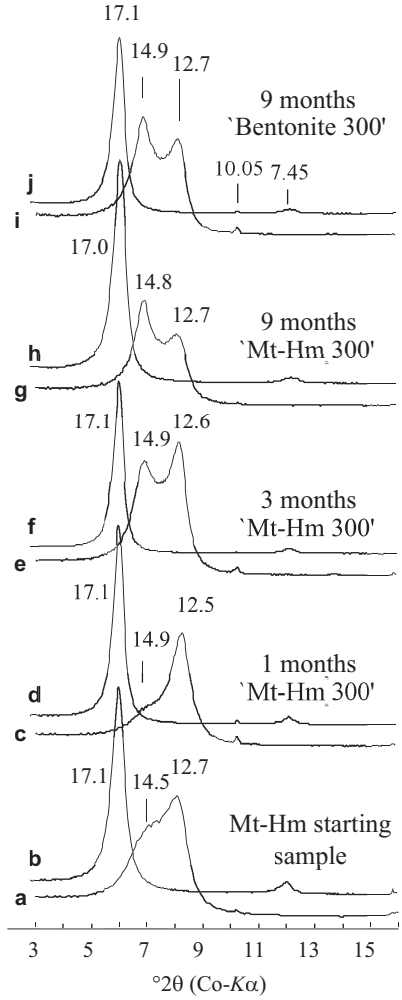

FIG. 3. XRD patterns of the Mt-Hm starting-sample, 1 month, 3 months and 9 months 'Mt-Hm 300' run samples, and 9 months 'Bentonite 300' run sample. (a, c, e, g, i) oriented air-dried; (b, d, f, h, j) EG-saturated. Reflection values in Å.

lines at 8.9 Å and 16.7 Å. This indicates that the starting smectite transformed to another mineral of the smectite group characterized by a significant tetrahedral charge deficiency (beidellite and/or saponite). The relative evolution of the 9.3 and 17 Å reflections indicates that the transformation is almost complete after 9 months.

A starting sample which was K saturated, heated at 110ºC overnight and EG saturated expands to 16.7 Å because of its low charge (0.38). After the same treatment, the 9 months run sample expands

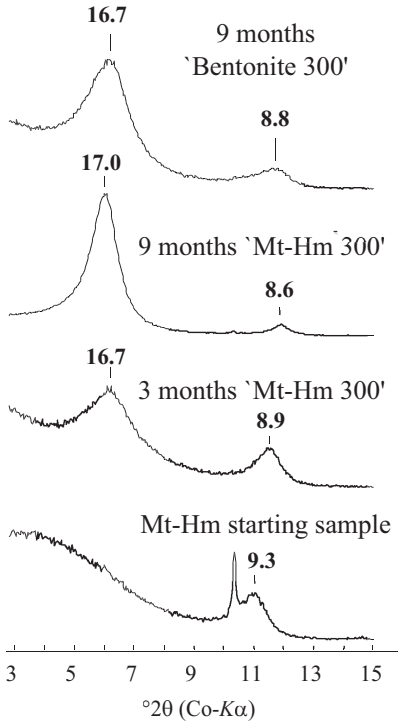

FIG. 4. XRD patterns of the Mt-Hm starting sample, 3 months and 9 months 'Mt-Hm 300' run samples, and 9 months 'Bentonite 300' run sample, after Greene-Kelly test. Reflection values in Å.

to 13.9 Å, indicating that the low-charge starting smectite is replaced by a high-charge smectite.

A 9 months run sample which was Mg saturated and then glycerol saturated expands, however, to 17 Å. This indicates that the clay phase is not of vermiculite type.

Some XRD patterns were obtained from powder specimens in the range 70−75º2θ (Fig. 1). We observe a decrease in the intensity of the reflection line of dioctahedral smectite (1.49 Å), and a shoulder is observed on the left hand side of the reflection line of quartz (1.54 Å) in the 9 months run sample, indicating the presence of a trioctahedral smectite.

XRD − transformation of the montmorillonite in other experiments. The 9 months 'Bentonite 300' run-sample shows the same type of transformation as the 9 months 'Mt-Hm 300' run sample. The XRD patterns from the Greene-Kelly test show a 16.7 Å peak and a small peak at 8.8 Å attributed to a smectite with tetrahedral charge deficiency and a residual amount of the starting montmorillonite, respectively. The XRD powder pattern of the same sample in the range 70−75º2θ (Fig. 1) confirms the presence of dioctahedral smectite (1.49 Å) and small amounts of trioctahedral smectite, as indicated by the shoulder on the left hand side of the quartz reflection line (1.54 Å).

The 'Bentonite 80' and 'Mt-Hm 80' run-samples obtained from experiments at 80ºC show no significant evolution of the clay phase (Table 3).

CEC

The results of the CEC measurements for starting and run samples are summarized in the Table 1. No significant evolution of the CEC is detected during the thermal treatment, regardless of the experimental conditions.

Crystal-chemistry of the clay phase

Determination of the Fe^{3+}/Fe_{tot} ratio by TMS. ^{57}Fe Mössbauer spectroscopy is the most efficient method by which to characterize the Fe species in solid phases. Mössbauer work on the 'environmental' materials has been mainly concerned with Fe in two mineral groups: clay-sized phyllosilicates (often looked upon as clay minerals *sensu stricto*) and oxides. Ideally, a distinction of Fe in these two groups by Mössbauer spectroscopy is relatively straightforward: the phyllosilicates are paramagnetic at room temperature and may contain both divalent and trivalent Fe, whereas the most common Fe oxides should be magnetically ordered and contain only trivalent Fe, except for magnetite which is the only pure oxide of mixed valence (Murad, 1998).

The Fe^{3+}/Fe_{tot} ratio in the clay phase was calculated from Mössbauer spectra for the 3 and 9 months 'Mt-Hm 80' and 'Mt-Hm 300' run samples. The results are reported as a function of time in Fig. 5. In the starting clay phase, the Fe^{3+}/Fe_{tot} ratio was 0.55 (Guillaume *et al*., 2001*b*). Two distinct trends are observed as a function of temperature: (1) at 300ºC, the Fe^{3+}/Fe_{tot} ratio decreases to 0.4 after 3 months, and to 0.3 after 9 months; (2) at 80ºC, in the 9 months run sample, the Fe^{3+}/Fe_{tot} ratio increases to a value of 0.9. It was not possible to determine precisely the Fe^{3+}/Fe_{tot} ratio in the 3 months 'Mt-Hm 80' run sample. In this sample, the amount of Fe as Fe oxides remains too high compared with the amount of Fe in the clay phase and the fitting of the spectrum was not possible.

Crystal-chemical changes of the run samples (EDS). Structural formulae of clay phases were calculated from EDS analyses, taking into account the results obtained by TMS for the Fe^{3+}/Fe_{tot} ratio. The clay particles were selected randomly for EDS analysis. Consequently, analytical points presented on the graphs do not necessarily represent, in a statistical manner, the various populations (unreacted smectite or newly formed particles). All structural formulae have been calculated on the basis of 11 oxygens as for the reference minerals (both di- and tri-octahedral clays: montmorillonite, beidellite, nontronite, saponite). All figures show the totality of analytical data for each run sample, in diagrams calculated on the basis of 11 oxygens. Selected compositions (in wt.% of elements) of the 9 months run samples are reported in Table 4.

The graphs presented in Figs 6 and 7 show the evolution of some cation-site occupancies of the run samples. The scatter of the analytical points for each run sample indicates a chemical heterogeneity, which may be due to mechanical mixing of inherited or partly transformed particles with new clay phases even at the smallest scale. The main changes in clay-particle composition are the following:

Tetrahedral site: in both the 'Bentonite 80' and 'Mt-Hm 80' run samples, a slight decrease in the Si content was observed (Fig. 6). In the 'Bentonite 300' run samples, a wide range of Si content is obtained with values ranging from 4 down to 3.7. In the 'Mt-Hm 300' run samples, the same evolution is observed and the Si content decreases down to a value of 3.2 for the longest duration.

Octahedral site: in both the 'Bentonite 80' and 'Mt-Hm 80' run samples, no significant evolution of the Fe and Mg contents was observed (Fig. 7). In the 'Bentonite 300' run samples, a slight increase in both Fe and Mg contents was observed in some particles. In the 'Mt-Hm 300' run samples, Fe and Mg contents increase significantly and both reach the value of 1 for some particles formed after the longest duration of experiment.

The overall evolution of the run products is well discriminated in the diagram (Fe^{3+},Al^{VI}) *vs*. (Mg,Fe^{2+}) (Fig. 8). Neither 'Bentonite 80' nor 'Mt-Hm 80' run samples showed any significant evolution. For 300ºC experiments, a trend is observed from the dioctahedral smectite domain which characterizes the starting montmorillonite, towards the trioctahedral smectite domain. This evolution is more significant for 'Mt-Hm 300' than for 'Bentonite 300' run samples.

The overall evolution of the clay in the 'Bentonite 300' and 'Mt-Hm 300' run-samples, especially the increasing tetrahedral charge shown by Figs 6, 7 and 8 can be explained by a change in the nature of the expandable layers from montmorillonite to high-charge trioctahedral smectite. This is in agreement with the preliminary interpretation of the XRD data. Mechanical mixing or mixed-layering between the starting dioctahedral smectite and the high-charge trioctahedral smectite are probably the main cause of the large compositional range of the run products. According to the compositional fields in the diagrams, the Fe^{3+}/Fe_{tot} ratio and the XRD results, the high-charge trioctahedral smectite is interpreted as an Fe saponite. In the 'Bentonite 80' and 'Mt-Hm 80' run samples, the lack of significant evolution in both Si *vs*. I.C. (interlayer cations) and Fe *vs*. Mg diagrams (Figs 6 and 7) is in agreement with the interpretation of the XRD results.

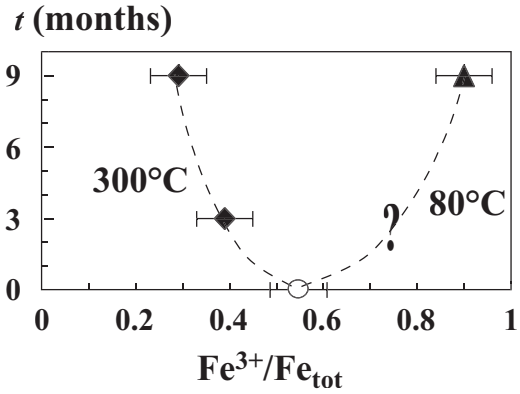

FIG. 5. Evolution of the Fe^{3+}/Fe_{tot} ratio in the clay phase of the run samples measured by TMS *vs*. experimental duration. Dark diamonds: 'Mt-Hm 300' experiments; dark triangle: 'Mt-Hm 80' experiment; open circle: comparison with the Fe^{3+}/Fe_{tot} ratio in the starting montmorillonite (Guillaume *et al*., 2001b).

Solution chemistry

Data on available experimental solutions are summarized in Table 5. The pH and Eh measured after cooling (at room temperature) and filtration of the experimental solution are presented as a function of the experiment duration in Fig. 9. The presence of Fe oxides in the experiments has no significant influence on the measured pH and Eh. At 80ºC, the run-solution pH decreases from 8.4

TABLE 4. Selected compositions (EDS analyses, in wt.% of elements) of the 9 months run samples.

Si	Al	Fe	Mg	K	Na	Ca	Si	Al	Fe	Mg	K	Na	Ca
Bentonite 80							Bentonite 300						
62.9	24.2	5.0	3.7	0.2	3.1	0.9	64.2	26.1	3.2	2.3	0.7	2.0	1.4
62.7	22.8	5.7	4.8	0.4	2.6	1.1	61.9	27.6	4.0	3.0	0.3	2.1	1.1
62.4	23.3	6.0	4.3	0.4	2.4	1.2	61.3	27.4	3.7	3.1	0.5	2.4	1.5
62.2	24.2	4.5	4.4	0.2	3.5	0.8	61.2	27.2	4.2	3.1	0.5	2.5	1.3
62.0	24.6	4.8	4.4	0.3	3.1	0.9	61.1	25.9	4.5	3.4	0.5	2.7	1.9
61.8	23.9	5.1	4.6	0.4	3.2	0.9	60.8	27.9	3.6	2.8	0.3	2.9	1.7
61.7	25.0	4.9	3.8	0.4	3.3	1.0	59.7	26.0	4.2	3.5	0.3	4.6	1.6
61.5	24.1	5.0	4.3	0.3	3.6	1.1	59.6	27.7	4.3	3.5	0.4	3.1	1.4
61.4	24.8	5.6	4.3	0.0	2.9	1.0	59.5	27.0	4.6	4.3	0.5	2.8	1.3
61.0	25.4	3.8	4.8	0.6	3.5	0.9	58.7	24.7	5.8	5.0	0.4	4.0	1.3
Mt-Hm 80							Mt-Hm 300						
63.1	23.2	5.3	4.1	0.3	2.8	1.2	58.6	30.1	3.1	3.2	0.5	3.1	1.5
62.6	25.2	2.8	5.0	0.1	3.5	0.8	57.2	28.4	5.9	3.7	0.0	2.7	2.1
62.5	24.9	2.5	5.4	0.2	4.0	0.5	56.8	28.7	5.6	4.3	0.0	3.1	1.5
62.2	25.4	2.7	5.1	0.0	3.6	0.9	53.8	26.6	8.5	6.2	0.5	2.7	1.7
62.1	23.5	6.1	4.3	0.3	2.4	1.2	52.5	26.6	8.6	6.0	0.0	4.4	2.0
62.0	22.9	5.5	4.8	0.4	3.0	1.4	47.8	23.1	14.8	8.8	0.0	3.8	1.6
61.9	23.1	5.3	4.9	0.4	3.0	1.2	40.4	17.1	25.7	12.7	0.4	1.9	1.6
61.4	24.2	5.3	4.5	0.4	3.0	1.0							
60.9	23.5	6.1	5.0	0.5	3.2	0.9							
60.8	24.1	6.3	4.3	0.4	3.1	1.0							

(starting solution pH) to 7.6 for the 3 months experiments, and then remains the same for the 9 months experiments. Eh decreases from +117 mV (starting solution Eh) to +31 mV for the 1 month experiment, and to ~+80 mV for the 3 months and 9 months experiments. At 300ºC, the run-solution pH decreases to a value of 6.3 and then remains almost constant after 1 month. Eh decreases significantly from +117 mV to ~−250 mV in 3 months and then increases almost to 0 mV for the 9 months experiments.

The evolution with time of the composition of the run solutions is presented as a function of the experiment duration in Fig. 10. The starting solution (after reacting with the bentonite at 25ºC) had a Na^+/Ca^{2+} ratio of ~75 (±2), regardless of the presence of added Fe oxides. In the case of 'Bentonite' samples, the Na^+/Ca^{2+} ratio is in the range 60−80, and in the case of 'Mt-Hm' samples, ranges from 50 to 60 at 80ºC, and from 60 to 110 at 300ºC. These changes in the Na^+/Ca^{2+} ratio are probably the result both of exchange processes and uptake by framework silicates like feldspars and zeolites. The Cl^- content can be considered as almost constant in 'Mt-Hm 300' samples. In the other cases, a significant decrease from 1200 to 500−600 ppm is observed, although no significant Cl^- incorporation in minerals has been determined. Cl^- is not fractionated by mineralogical changes and is usually considered a conservative element. The depletion in Cl^- content is therefore not fully explained in our case.

Evolution of Si concentration is distinct at 80 and 300ºC, regardless of the 'Bentonite' or 'Mt-Hm' experiments. At 80ºC, the Si concentration is ~60 ppm after 3 months, close to the saturation with respect to quartz. It decreases to ~45 ppm for experiments of longer duration. At 300ºC, Si concentration increases to 500 ppm after 1 month, close to saturation with respect to quartz, and decreases to 80 ppm for experiments of longer duration. The significant silica release suggests the dissolution of smectite layers, and the subsequent increase in silica concentrations to the saturation of the solution with respect to quartz. The significant decrease in Si concentration down to 45 ppm (80ºC experiments) and 80 ppm (300ºC experiments) is not well understood.

The concentrations of Al, Fe and Mg in the experimental solutions, display similar evolutions

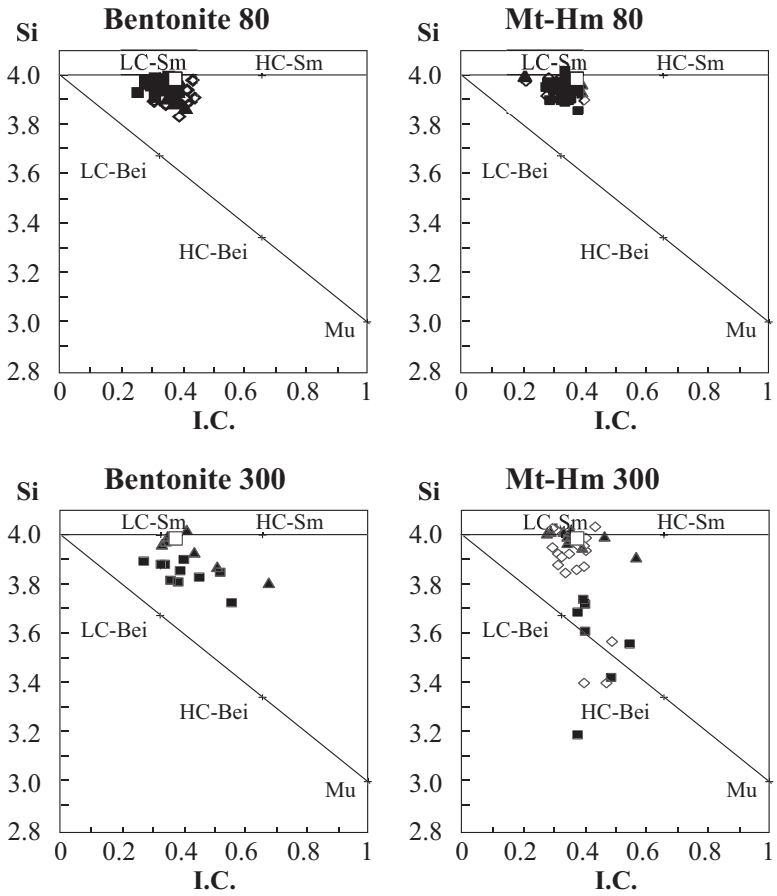

FIG. 6. Chemistry of the clay phase of the starting sample (open square), 1 month (filled triangles), 3 months (open diamonds) and 9 months (filled squares) run samples. Si *vs*. interlayer cations (I.C. = Na+2Ca+K), from structural formulae calculated on the basis of 11 oxygens. Reference minerals are reported: low-charge and high-charge smectite (LC-Sm, HC-Sm), low-charge and high-charge beidellite (LC-Bei, HC-Bei), Muscovite (Mu).

with time: an increase during the first week followed by a decrease for longer duration in both 'Bentonite' and 'Mt-Hm' run samples, and higher for 80ºC than 300ºC experiments. The presence of Mg, Al and Fe in the solution during the first week suggests a partial dissolution of smectite. For the longest durations, the very weak concentrations of Mg, Al and Fe indicate significant uptake by the newly formed clays, zeolites and feldspars.

DISCUSSION

Evolution of added Fe-bearing phases

Iron oxides (hematite, magnetite) added to the experimental system are stable under the experimental conditions as shown by XRD and SEM data. The starting hematite and magnetite powders dissolve, however, in favour of large crystals following the Ostwald ripening principle (Kang *et al*., 2002).

Newly formed non-clay minerals: quartz, feldspar and zeolite

The SEM and XRD data demonstrated the formation of new quartz, feldspar and zeolite. Other non-clay minerals that were present in the starting bentonite are consumed. These series of dissolution-precipitation processes occurred rapidly, and were enhanced by the presence of added Fe oxides, especially at 300ºC.

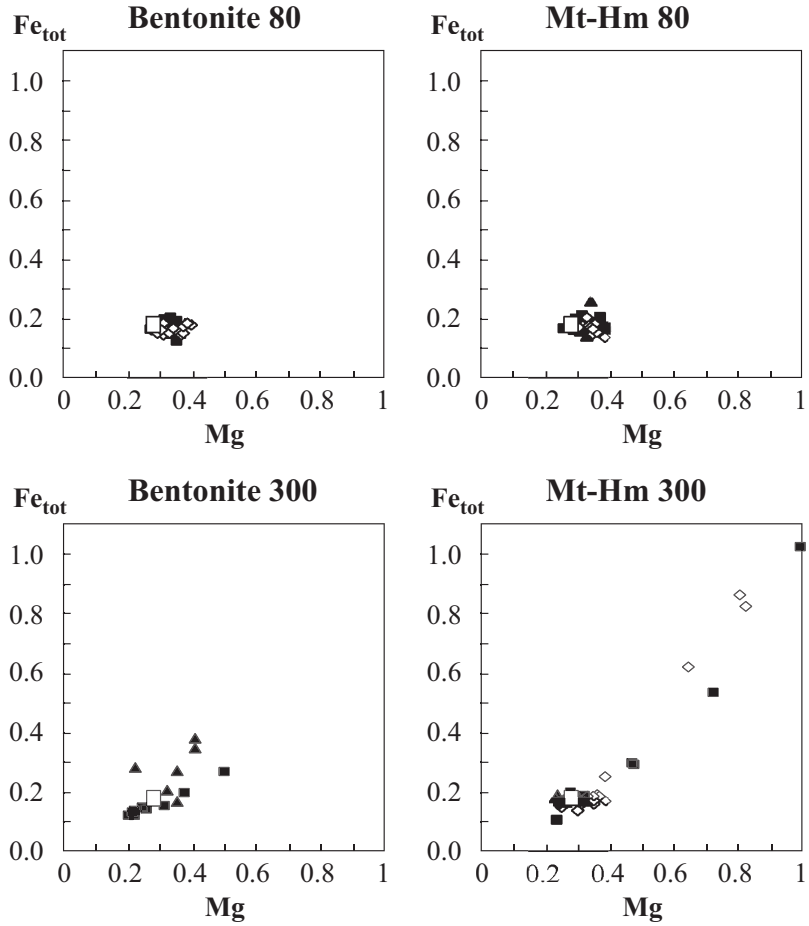

FIG. 7. Chemistry of the clay phase of the starting sample (open square), 1 month (filled triangles), 3 months (open diamonds) and 9 months (filled squares) run samples. Fe total *vs*. Mg, from structural formulae calculated on the basis of 11 oxygens.

Conversion of the starting montmorillonite into newly formed clays, poorer in silica, results in a release of Si to the solution. The excess silica crystallizes as subhedral quartz crystals. Semi-quantitative estimation of the volume of quartz produced by the reaction is in a good agreement with the calculated volume of quartz, which can be formed after release of silica during the dissolution-crystallization process: equations written at constant Al and using the structural formulae of the starting and run products indicate that one mole Na/Ca-smectite may transform approximately into 1.1 moles of saponite and 0.35 moles of quartz (if the formation of feldspar and zeolite is not taken into account for the Si excess).

Newly formed clay phases

On the basis of XRD, CEC, TMS and EDS data, hydrothermal treatment of the bentonite at 300ºC resulted in the partial conversion of montmorillonite to saponite. Partly transformed particles are detected by their intermediate compositions as shown by EDS. This transformation is accompanied by a decrease in the Fe^{3+}/Fe_{tot} ratio in the clay phase, the newly formed saponite being Fe^{2+}-rich. The presence of hematite and magnetite powders in the experimental system enhances reactions although it has been demonstrated that these minerals are stable in the conditions of the experiments. At 80ºC, the montmorillonite is stable at the time scale of our experiments and

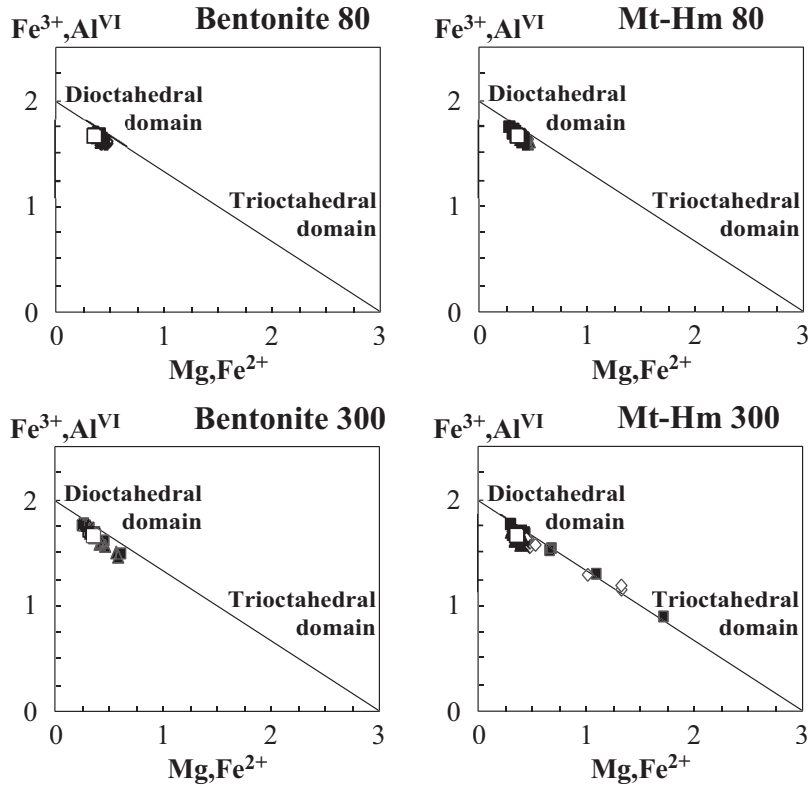

FIG. 8. Chemistry of the clay phase of the starting sample (open square), 1 month (filled triangles), 3 months (open diamonds) and 9 months (filled squares) run samples. (Fe^{3+},Al^{VI}) *vs*. (Fe^{2+},Mg), from structural formulae calculated on the basis of 11 Oxygens.

shows very slight evolution, except for the increase of the Fe^{3+}/Fe_{tot} ratio to 0.9.

Evolution of the solution chemistry

The increase of Si, Fe, Mg and Al content in the run solution during the first weeks of experiments in relation to the dissolution of starting minerals is followed by a strong decrease in element concentrations, in agreement with the precipitation of saponite, quartz, feldspars and zeolite. The evolution of the Eh-pH of the solution is in good agreement with the evolution of the Fe^{3+}/Fe_{tot} ratio in the clay phase as measured by TMS in experiments with added Fe oxides. At 80ºC, the system became oxidizing and the Fe^{3+}/Fe_{tot} ratio in the clay phase increased to 0.9. At 300ºC, the conditions were more reducing and the Fe^{3+}/Fe_{tot} ratio in the clay phase decreased to 0.3.

Comparison with natural systems and previous works

The formation of quartz, feldspars and zeolites as reaction products of the smectite-Fe oxides-chloride solution system is consistent both with thermodynamic modelling predictions (Cathelineau *et al*., 2001) and with other experimental data. Feldspars were commonly observed among reaction products in hydrothermal experiments on Na- and K-montmorillonite between 260 and 400ºC (Eberl & However, 1977; Eberl, 1978). Inoue (1983) reported the formation of Ca-zeolites (wairakite and heulandite) as well as illite and smectite, from the reaction of Ca-montmorillonite with 0.2 mol l^{-1} KOH at 300ºC. In addition, zeolites and feldspars associated with smectite are commonly observed in alteration products of volcanic glasses and basic magmatic rocks submitted to hydrothermal altera-

TABLE 5. Chemistry of the initial, starting (after 6 days' equilibrium) and run solutions.

Sample		pH	Eh (mV)	Si	Al	Fe	Mg	Ca	Na	K	Cl	Na/Ca
Initial solution		6.4	121	0	0	0	0	200	632	0	1032	5.5
'Bentonite' samples												
25ºC	starting	8.4	117	16	0	1	7	26	1104	22	1053	74
80ºC	1 day	n.a.	n.a.	21	6	0	14	19	785	88	1261	71
	1 week	n.a.	n.a.	42	14	1	17	26	807	107	1113	55
	1 month	8.2	31.5	58	0	0	10	42	1326	36	n.a.	56
	3 months	7.5	78	63	0	0	7	32	1173	23	n.a.	65
	3 months	7.5	76	59	0	0	7	31	1287	43	n.a.	72
	9 months	7.5	79.6	44	0	0	8	45	1246	33	408	48
	9 months	7.6	84.6	44	0	0	6	48	1264	36	414	46
300ºC	1 month	6.2	−224	516	1	2	1	27	1160	55	n.a.	75
300ºC	9 months	6.5	96.6	111	0	0	1	12	560	28	566	85
'Mt-Hm' samples												
25ºC	starting	8.5	79.5	16	0	0	7	26	1077	22	1077	73
80ºC	1 day	n.a.	n.a.	48	16	13	11	25	836	65	1340	59
	1 week	n.a.	n.a.	34	11	7	22	28	933	113	1091	58
	1 month	8.2	2	57	0	0	10	46	1280	33	n.a.	48
	3 months	7.3	104	58	0	0	7	33	1180	199	n.a.	63
	3 months	7.4	98	58	0	0	7	34	1324	47	n.a.	68
	9 months	7.5	83.6	43	0	0	6	47	1301	35	410	48
	9 months	7.4	89.6	45	0	0	9	45	1237	49	501	48
300ºC	1 week	n.a.	n.a.	372	2	n.a.	n.a.	13	708	72	1049	98
	1 month	6.4	−188	503	1	1	1	29	1198	60	n.a.	73
	3 months	6.5	−256	312	1	1	1	14	855	83	n.a.	106
	9 months	6.4	−3.4	69	0	0	1	22	1024	41	825	79
	9 months	6.4	8.6	63	0	0	1	28	823	48	1085	52

All concentrations in mg/l
n.a.: not analysed

tion (among others, Honnorez, 1981; Kastner, 1981; Cathelineau *et al.*, 1985; Alt *et al.*, 1986; Cathelineau & Izquierdo, 1988; Schiffman & Fridleifsson, 1991).

The evolution of the clay and other minerals in this study completes the results of Guillaume *et al.* (2003) which provide data on the system metallic Fe-magnetite-smectite at 300ºC. In these experiments conducted under similar conditions, the addition of metallic Fe (powder and plaque) + magnetite powder instead of magnetite + hematite powders leads to the formation of chlorite. This chlorite is Fe^{2+}-rich at the nearest contact of metallic Fe plaque but it has a higher Mg content in the absence of or far from the metallic Fe plaque. The formation of chlorite is also accompanied by the crystallization of quartz, feldspar and zeolite and dissolution of other trace minerals.

The overall consideration of these two sets of data indicates that the redox state of the system and the availability of Fe are two critical parameters which control the formation of the Fe-rich mineral phases such as chlorite or Fe-saponite, and their relative abundance.

CONCLUSIONS

Experiments at 300ºC resulted in mineralogical changes, such as the formation of Fe saponite, quartz, feldspar and zeolite, and a decrease in the Fe^{3+}/Fe_{tot} ratio in the clay phase.

At 80ºC, in the presence or not of added Fe oxides, the starting montmorillonite appears to be stable and no significant transformation is detected except an increase of the Fe^{3+}/Fe_{tot} ratio. Analyses of the solutions show that the system became more oxidizing and TMS data illustrated that the Fe^{3+}/Fe_{tot} ratio in the clay phase increased from 0.55 to 0.9, the smectite containing mostly Fe^{3+}. This observation indicates that the kinetics of Fe phase-solution

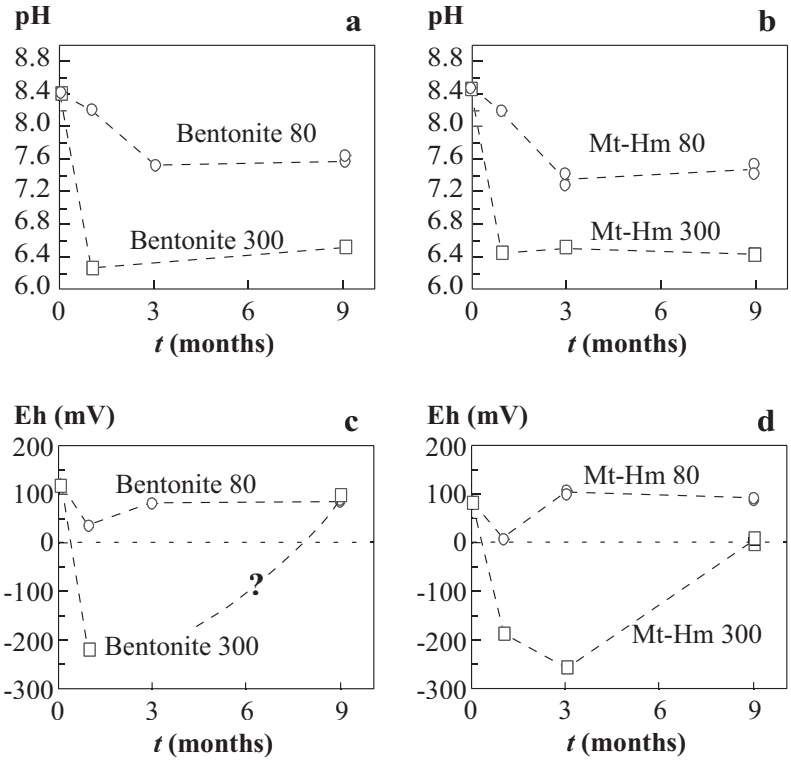

FIG. 9. Chemistry of the run solutions: (a–b) evolution of pH *vs*. time for 'Bentonite'- and 'Mt-Hm'-type experiments, respectively. (c–d) Evolution of Eh *vs*. time for 'Bentonite'- and 'Mt-Hm'-type experiments, respectively.

equilibrium was slow at 80ºC and during the experiments the system showed oxidizing behaviour.

At 300ºC, the redox conditions are far more reducing and yield lower Fe^{3+}/Fe_{tot} ratios in the clay phase, down to 0.3, the newly formed Fe-rich trioctahedral smectite containing mostly Fe^{2+}. Thus, the addition of Fe oxides in the system triggers reactions, including the formation of Fe-rich phases, which are more stable than the primary smectite. Results obtained at 300ºC also indicate that in some cases clay minerals can be considered as good markers of the evolution of the redox conditions.

The prediction of the potential behaviour of smectite in the presence of steel container and their related alteration products, under nuclear waste repository conditions, is made difficult by the consideration of the potential temperature range of the processes (25–90ºC, eventually 150ºC), e.g. a temperature below which very little mineralogical change can be determined. Experiments carried out at higher temperatures could eventually be extrapolated to lower temperatures using temperature-time consideration (Arrhenius kinetic laws), if the type of mineralogical change is thought to occur at much lower temperatures. The data obtained cannot answer fully the question of long-term behaviour at low temperatures: (1) the presence of Fe oxides at 80ºC does not affect the stability of the smectite for the experimental duration of 9 months, (2) at 300ºC, the montmorillonite of the starting bentonite is partly transformed to saponite. The realization of this mineralogical change at temperatures <300ºC still needs to be confirmed.

ACKNOWLEDGMENTS

Experiments were conducted at the Géologie et Gestion des Ressources Minérales et Energétiques laboratory (G2R, CNRS-CREGU-INPL-UHP, Vandœuvre-lès-Nancy, France). The XRD data were collected at the Laboratoire Environnement et Minéralurgie (LEM, CNRS-INPL, Vandœuvre-lès-Nancy, France), the

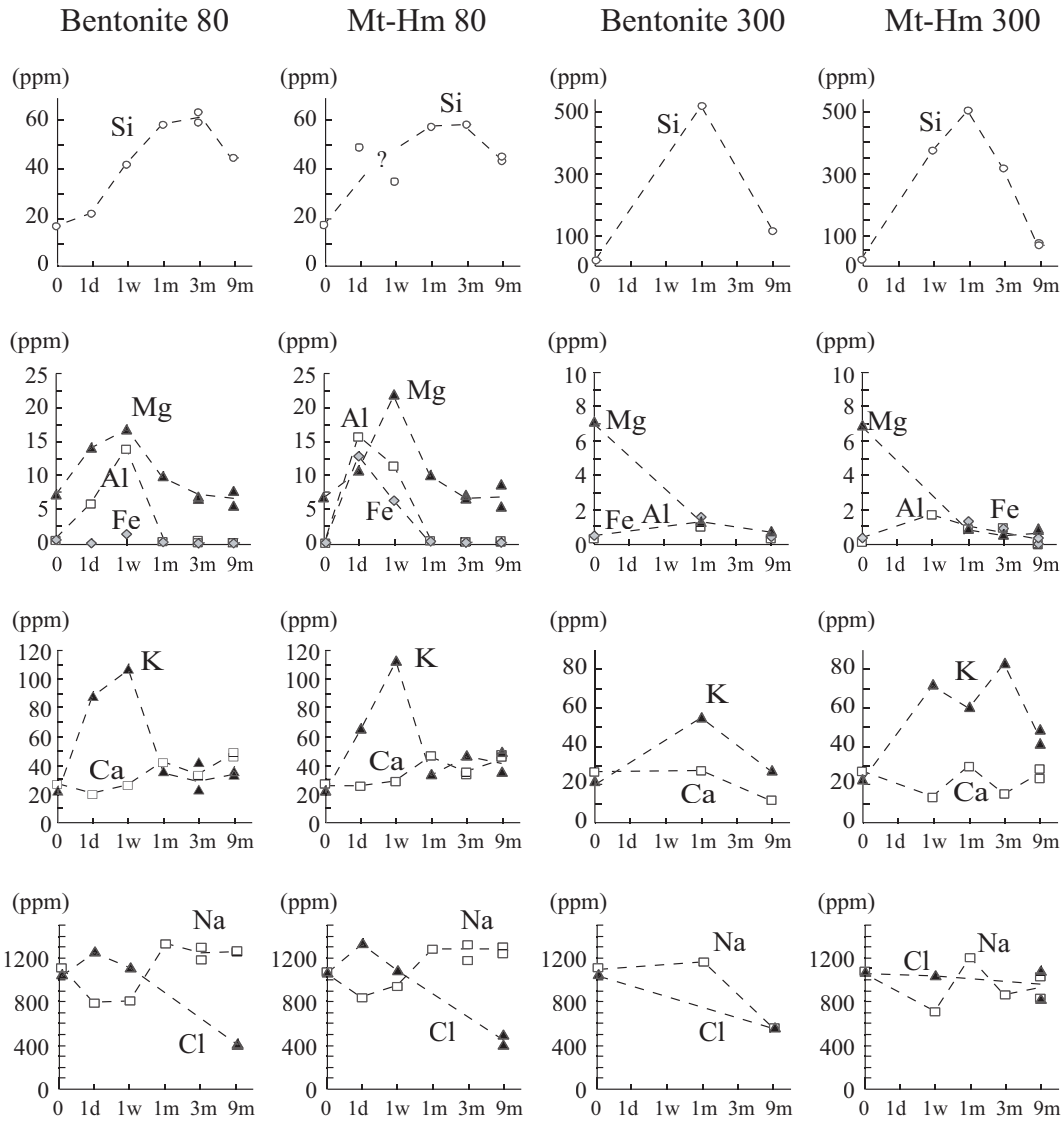

FIG. 10. Chemistry of the run solutions. Evolution with time of the solution composition (ppm scale) for different cations (Si, Al, Fe, Mg, K, Ca, Na and Cl) and the four different experimental conditions. 1d = 1 day, 1w = 1 week, 1m = 1 month, 3m = 3 months, 9m = 9 months.

SEM micrographs at the Université Henri Poincaré (Vandœuvre-lès-Nancy, France), the TMS performed at the Laboratoire de Chimie Physique et Microbiologie pour l'Environnement (LCPME, CNRS-UHP, Villers-lès-Nancy, France), the EDS-TEM at the Université Henri Poincaré (Vandœuvre-lès-Nancy, France), and the ICP-AES and ICP-MS analyses of solutions at the Centre de Recherches Pétrographiques et Géochimiques (CRPG, CNRS, Vandœuvre-lès-Nancy, France). The authors wish to thank J. Ghanbaja (UHP, Vandœuvre-lès-Nancy, France) for the EDS analyses and I. Bihannic and F. Lhote (LEM, Vandœuvre-lès-Nancy, France) for their help and technical assistance with XRD. This research was supported financially by Andra – Agence Nationale pour la gestion des Déchets RadioActifs (French National Agency for the Management of Radioactive Wastes) – in the framework of its project

on the geochemical behaviour of the bentonite engineered barrier. We thank A.G. Türmenoglu, J. Cuevas and A.M. Karpoff, the Associate Editor, for their constructive comments.

REFERENCES

Alt J., Honnorez J., Laverne C. & Emmerman R. (1986) Hydrothermal alteration of a 1 m section through the upper oceanic crust. Deep Sea Drilling project Hole 504B: mineralogy, chemistry and evolution of seawater-basalt interactions. *Journal of Geophysical Research*, **91**, 10, 309–335.

Benali O., Abdelmoula M., Refait P. & Génin J.M. (2001) Effect of orthophosphate on the oxidation products of Fe(II)-Fe(III) hydroxycarbonate: the transformation of green rust to ferrihydrite. *Geochimica et Cosmochimica Acta*, **65**, 1715–1726.

Buatier M., Honnorez J. & Ehret G. (1989) Fe-smectite-glauconite transition in the hydrothermal green clays from the Galapagos spreading center. *Clays and Clay Minerals*, **37**, 532–541.

Buatier M.D., Ouyang K. & Sanchez J.P. (1993) Iron in hydrothermal clays from the Galapagos spreading centre mounds: consequences for the clay transition mechanism. *Clay Minerals*, **28**, 641–655.

Buatier M.D., Früh-Green G.L. & Karpoff A.M. (1995) Mechanisms of Mg-phyllosilicate formation in a hydrothermal system at a sedimented ridge (Middle Valley, Juan de Fuca). *Contributions to Mineralogy and Petrology*, **122**, 134–151.

Byström-Brusewitz A.M. (1975) Studies of the Li test to distinguish beidellite and montmorillonite. *Proceedings of the International Clay Conference 1972, Mexico City*, Applied Publishing Ltd., Wilmette, Illinois, USA, Pp. 419–428.

Cathelineau M. & Izquierdo G. (1988) Temperature-composition relationships of authigenic micaceous minerals in the Los Azufres geothermal system. *Contributions to Mineralogy and Petrology*, **100**, 418–428.

Cathelineau M., Oliver R., Nieva D. & Garfias A. (1985) Mineralogy and distribution of hydrothermal mineral zones in Los Azufres (Mexico) geothermal field. *Geothermics*, **14**, 49–57.

Cathelineau M., Mosser-Ruck R. & Charpentier D. (2001) Interactions fluides/argilites en conditions de stockage profond des déchets nucléaires. Intérêt du couplage expérimentation/modélisation dans la compréhension des mécanismes de transformation des argiles et la prédiction à long terme du comportement de la barrière argileuse. Pp. 305–341 in: *Actes des Journées Scientifiques ANDRA, Nancy, France*. EDP Sciences.

Eberl D.D. (1978) Reaction series for dioctahedral smectites. *Clays and Clay Minerals*, **26**, 327–340.

Eberl D.D. & Hower J. (1977) The hydrothermal transformation of Sodium and Potassium smectite into mixed-layer clay. *Clays and Clay Minerals*, **25**, 215–227.

Eberl D.D., Whitney G. & Khoury H. (1978) Hydrothermal reactivity of smectite. *American Mineralogist*, **63**, 401–409.

Greene-Kelly R. (1953) The identification of montmorillonoids in clays. *Journal of Soil Science*, **4**, 233–237.

Guillaume D., Neaman A., Mosser-Ruck R., Dubessy J., Cathelineau M. & Villiéras F. (2001a) Experimental study of hydrothermal reactivity of bentonite at 80 and 300ºC in the presence of iron and/or iron oxides. Berichte der Deutschen Mineralogischen Gesellshaft, Beihefte zum *European Journal of Mineralogy*, **13**, p. 69 p.

Guillaume D., Pironon J. & Ghanbaja J. (2001b) Valence determination of iron in clays by electron energy loss spectroscopy. Berichte der Deutschen Mineralogischen Gesellshaft, Beihefte zum *European Journal of Mineralogy*, **13**, p. 70.

Guillaume D., Neaman A., Cathelineau M., Mosser-Ruck R., Peiffert C., Abdelmoula M., Dubessy J., Villiéras F., Baronnet A. & Michau N. (2003) Experimental synthesis of chlorite from smectite at 300ºC in the presence of metallic iron. *Clay Minerals*, **38**, 281–302.

Hoffmann U. & Klemen E. (1950) Loss of exchangeability of lithium ions in bentonites on heating. *Zeitschrift für Anorganische und Allgemeine Chemie*, **262**, 95–99.

Honnorez J. (1981) The aging of the oceanic crust at low temperature. Pp. 525–587 in: *The oceanic lithosphere. The Sea*, 7, (C. Emiliani, editor). Wiley Interscience Publishers, John Wiley & Sons, New York.

Inoue A. (1983) Potassium fixation by clay minerals during hydrothermal treatment. *Clays and Clay Minerals*, **31**, 81–91.

Kang M.K., Kim D.Y. & Hwang N.M. (2002) Ostwald ripening kinetics of angular grains dispersed in a liquid phase by two dimensional nucleation and abnormal grain growth. *Journal of the European Ceramic Society*, **22**, 603–612.

Kastner M. (1981) Authigenic silicates in deep sea sediments: formation and diagenesis. Pp. 915–980 in: *The oceanic lithosphere. The Sea*, 7, (C. Emiliani, editor). Wiley Interscience Publishers, John Wiley & Sons, New York.

Madsen F.T. (1998) Clay mineralogical investigations related to nuclear waste disposal. *Clay Minerals*, **33**, 109–129.

Müller-Vonmoos M., Kahr G., Bucher F., Madsen F.T. & Mayor P.A. (1991) *Untersuchungen zum Verhalten von Bentonit in kontakt mit Magnetit und Eisen unter Endlagerbedingungen*. NTB 91–14.

Nagra, Hardstrasse 73, CH-5430 Wettingen, Switzerland.

Murad E. (1998) Clays and clay minerals: What can Mössbauer spectroscopy do to help understand them? *Hyperfine Interactions*, **117**, 39–70.

Schiffman P. & Fridleifsson G.O. (1991) The smectite-chlorite transition in drillhole Nj-15, Nesjavellir geothermal field, Iceland: XRD, BSE, and Electron Microprobe Investigations. *Journal of Metamorphic Geology*, **9**, 679–696.

Yamada H., Yoshioka K., Tamura K., Fujii K. & Nakazawa H. (1998) Reaction sequences of sodium montmorillonite under hydrothermal conditions. *Clay Science*, **10**, 385–394.